3D laser measurement system for large scale architectures using multiple mobile robots

Ryo Kurazume, Yukihiro Tobata, Yumi Iwashita, and Tsutomu Hasegawa
Kyushu University
744, Motooka, Nishi-ku, Fukuoka, 819-0395, JAPAN
kurazume@is.kyushu-u.ac.jp

Abstract

In order to construct three dimensional shape models of large scale architectures by a laser range finder, a number of range images are normally taken from various viewpoints and these images are aligned using post-processing procedure such as ICP algorithm. However in general, before applying ICP algorithm, these range images have to be registered to correct positions roughly by a human operator in order to converge to precise positions. In addition, range images must be overlapped sufficiently each other by taking dense images from close viewpoints. On the other hand, if poses of the laser range finder at viewpoints can be identified precisely, local range images can be converted to the world coordinate system directly with simple transformation calculation. This paper proposes a new measurement system for large scale architectures using a group of multiple robots and an on-board laser range finder. Each measurement position is identified by the highly precise positioning technique named Cooperative Positioning System or CPS which utilizes the characteristics of multiple robots system. The proposed system can construct 3D shapes of large scale architectures without any post-processing procedure such as ICP algorithm and dense range measurements. The measurement experiments in unknown and large indoor/outdoor environments are successfully carried out using the newly developed measurement system consisting of three mobile robots named CPS-V.

1. Introduction

Aiming at preserving 3D shapes or views of cultural heritages using laser range finders or digital cameras, several research projects are being promoted such as "The Digital Michelangelo Project"[8], Angkor[5] and Tzuchingch'eng Palace[1]. Generally, for constructing 3D models of these large scale architectures, since a laser range finder cannot cover the whole area at once due to the limitation of measurable distance and occlusion problems, a number of range images are normally taken from various viewpoints and these images are aligned using post-processing procedures such as ICP algorithm[2],[3]. After post-processing procedures, range images described in the sensor coordinate system are transformed to the world coordinate system and the whole shape of the architecture is obtained. However in general, before applying ICP method, it is necessary to register range images to correct positions roughly by a human operator in order to converge to proper positions. This procedure is quite laborious and time-consuming, and is considered as a significant obstacle for developing an automatic 3D laser measurement system. In addition, in order to register range images precisely by ICP algorithm, all the images must contain a plenty of feature shapes and overlap sufficiently each other by scanning densely from a number of positions.

On the other hand, another approach with no post-processing procedures can be considered, that is, the identification of the pose of the range sensor precisely at each measurement. Since this method can obtain the transformation matrix from the sensor specific coordinate system to the world coordinate system, local range images are converted to the world coordinate system directly with simple transformation calculation, and no post-processing procedures such as the ICP algorithm are required. As an example of this approach, several systems have been proposed so far which utilizes the GPS [12],[10] for determining the position of the range sensor. However, special instruments and techniques such as RTK (Real-time Kinematic) system or VRS (Virtual Reference Station) method are requisite for achieving highly precise position identification by current GPS. Moreover, GPS cannot be used if enough numbers of satellites cannot be seen, for example, in a narrow space in architectures, forest, or an indoor environment.

This paper proposes a new 3D measurement system for large scale architectures using a group of mobile robots and an on-board laser range finder. This system utilizes the Co-

operative Positioning System (CPS)[7] for multiple robots, which has been proposed as a highly precise position identification technique for mobile robots. By combining highly precise position identification by CPS and an on-board laser range finder, an automatic measurement system for large scale architectures is realized. This system can construct a 3D shape of large scale architecture without any post-processing procedures such as ICP algorithm. In addition, it is also possible to register range images even if number of measurements is few and sparse range images are only available, or feature shapes or overlapped regions are not contained sufficiently in range images. It is also possible to construct a 3D model in an environment where GPS is not available such as inside of architecture or an indoor environment. The proposed system strongly relates to the SLAM (simultaneous localization and mapping) [9],[11],[4] which is attracting much attention in robotics community. We think it is possible to utilize the system with the aim of the localization and mapping of mobile robots.

2 Precise positioning of mobile robots

Let's consider the system in which a mobile robot equipped with an on-board laser range finder moves around a measurement target, and scans the target from many positions. If all the measurement positions are identified with high accuracy, range data acquired at each position can be converted to the world coordinate system by simple coordinate transformation calculation.

Several position identification methods have been proposed so far, and these methods can be classified into three categories.

1. Integrate sensor output from internal sensors such as an encoder at a wheel or an acceleration sensor.

2. Observe external landmarks by external sensors such as a laser range finder or a camera.

3. Use Global Positioning System, GPS.

The method (1) is called as odometry or dead reckoning method, and quite popular positioning technique especially for a wheeled vehicle. However, there are some drawbacks in this method, for example, the accuracy of position identification in uneven terrain is quite low due to the slippage of wheels, and 3D positioning including elevation is impossible. The method (2) has high accuracy if landmarks placed on the moving path can be measured precisely. However, landmarks have to be placed beforehand along the moving path and the precise map of these landmarks has to be available. Therefore, the method (2) cannot be used in unknown environment. The method (3) can be considered as a special case of the method (2) and is becoming very popular especially for field robots. However, this method also has several drawbacks, for example, active fields of robots are limited to an outdoor environment without obstacles toward satellites, and the accuracy is not so high in current technology except using some special techniques explained in Section I.

To overcome these limitations of position identification problems and realize accurate positioning for mobile robots, Kurazume et al. have proposed Cooperative Positioning System or CPS. In this system, multiple robots with highly precise measurement devices of mutual positions are controlled cooperatively, and incomparable accurate positioning is realized even in unknown and uneven environments against conventional positioning techniques. This section introduces the basic principle of CPS and the example of SLAM (Simultaneous Localization And Mapping) using CPS.

2.1 Cooperative Positioning System, CPS

The basic principle of CPS is as follows: We divide the robots into two groups, A and B. One group, A, remains stationary and acts as a landmark while group B moves. Group B then stops and acts as a landmark for group A. This "dance" is repeated until the target position is reached. By using the concept of "portable landmarks", CPS has a far lower accumulation of positioning error than dead reckoning, and can work in three-dimensions which are not possible with dead reckoning. In addition, since there is no need to place landmarks beforehand, CPS can be used in unknown environment.

An example of CPS is shown in Fig.1. This example is for a robot system consisting of a parent robot with a sensing device such as a laser range finder and two child robots. The sensing device can measure the relative positions of the child robots from the parent robot. Firstly, we assume that the initial position of the parent robot is measured or defined beforehand.

(1) The child robots 1 and 2 are moved and stopped.

(2) The parent robot measures the distance, azimuth, and elevation angles to the child robot 1 and identifies the position of the child robot 1.

(3) In the same as step 2, the position of the child robot 2 is identified.

(4) The parent robot moves and stops. Then the distances, azimuth, and elevation angles to the child robots 1 and 2 are measured and the position of the parent robot is calculated using the triangular surveying technique.

(5) Repeat from steps 1 to 4 until the target position is reached.

An example of positioning experiments by CPS in an outdoor environment is shown in Figs.2 and 3. The positioning error after long distance movement of 323.9m including the difference of elevation of 10m was 0.97m (0.3% of the total distance). This positioning accuracy is quite high comparing with other conventional techniques.

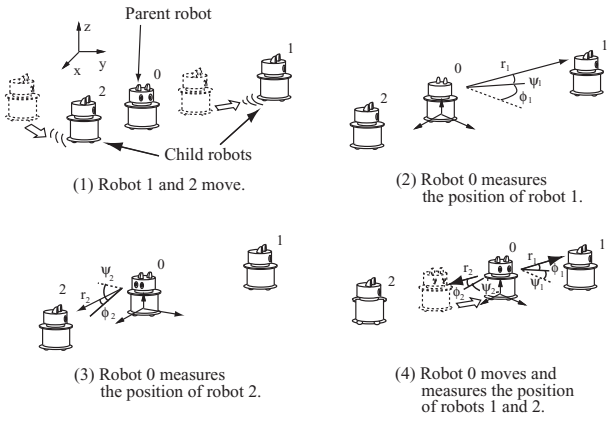

Figure 1. Cooperative Positioning System, CPS

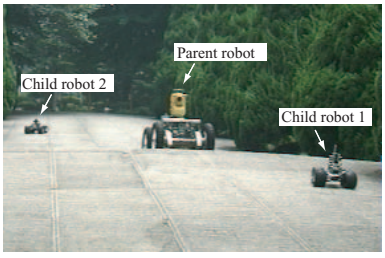

Figure 2. Long distance measurement experiments

2.2 Positioning accuracy of CPS

We discuss analytically about the positioning accuracy of CPS in this section. Let's consider CPS consisting of three robots as shown in Fig.1. Firstly we discuss the case that the position of the parent robot 0 is identified by measuring the distances, azimuth, and elevation angles to the child robots 1 and 2 as shown in Fig.1(4). The positions of robots are defined as $\mathbf{P}_i(x_i, y_i, z_i, \theta_i)$,$(i = 0 \sim 2)$. The distance from the robot 0 to the robots 1 and 2 are r_1, r_2, and the azimuth and elevation angles to the robots 1 and 2 are ϕ_1,ϕ_2,ψ_1, and ψ_2, respectively. The observation equations in this case are given by the following equations.

$$(x_0 - x_1)^2 + (y_0 - y_1)^2 = r_1^2 \cos^2 \psi_1 \quad (1)$$

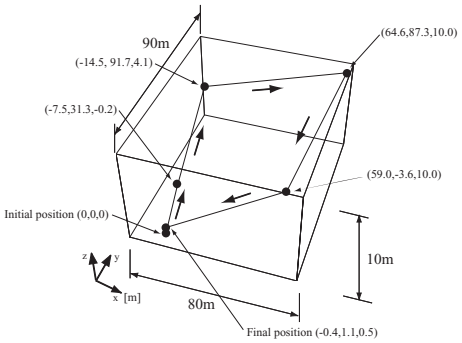

Figure 3. Results of long distance measurement experiments

$$(x_0 - x_2)^2 + (y_0 - y_2)^2 = r_2^2 \cos^2 \psi_2 \quad (2)$$

$$z_0 = z_1 - r_1 \sin \psi_1 \quad (3)$$
$$= z_2 - r_2 \sin \psi_2 \quad (4)$$

$$\theta_0 = -\phi_1 + \tan^{-1} \frac{y_1 - y_0}{x_1 - x_0} \quad (5)$$
$$= -\phi_2 + \tan^{-1} \frac{y_2 - y_0}{x_2 - x_0} \quad (6)$$

Here, since the variables to be determined are the position of the robot 0, $\mathbf{P}_0(x_0, y_0, z_0, \theta_0)$, this system has redundancy. Therefore, by substituting $x_i = \tilde{x}_i + dx_i$ into the above equations and using Taylor expansion, the following equation is derived.

$$\mathbf{A}\mathbf{X}_0 = \mathbf{L} + \mathbf{K}_1\mathbf{X}_{1,2} + \mathbf{K}_2\mathbf{\Theta} \quad (7)$$

where $\mathbf{X}_0 = (dx_0\ dy_0\ dz_0\ d\theta_0)^T$,
$\mathbf{X}_{1,2} = (dx_1\ dy_1\ dz_1\ d\theta_1\ dx_2\ dy_2\ dz_2\ d\theta_2)^T$, $\mathbf{\Theta} = (dr\ d\phi\ d\psi)^T$ (dr,$d\phi$, and $d\psi$ are measurement errors and we assume $dr = dr_i$ etc.),

$$\mathbf{L} = \begin{pmatrix} \tilde{r_1}\cos\tilde{\psi}_1 - d_1 \\ \tilde{r_2}\cos\tilde{\psi}_2 - d_2 \\ \tilde{z_1} - \tilde{r_1}\sin\tilde{\psi}_1 - \tilde{z_0} \\ \tilde{z_2} - \tilde{r_2}\sin\tilde{\psi}_2 - \tilde{z_0} \\ \tilde{\phi}_1 + \tilde{\theta}_0 - \tan^{-1}\frac{\tilde{y_1}-\tilde{y_0}}{\tilde{x_1}-\tilde{x_0}} \\ \tilde{\phi}_2 + \tilde{\theta}_0 - \tan^{-1}\frac{\tilde{y_2}-\tilde{y_0}}{\tilde{x_2}-\tilde{x_0}} \end{pmatrix} \quad (8)$$

and $\mathbf{A} \in R^{6\times4}$, $\mathbf{K}_1 \in R^{6\times8}$, $\mathbf{K}_2 \in R^{6\times3}$ are all coefficient matrices.

Next, by considering the case that all the elements of $\mathbf{L}$ which indicates the observation error are 0, the square error of the right part of Eq.(7), that is, the error variance matrix is calculated as follows:

$$\mathbf{\Sigma}_L = \mathbf{K}_1\mathbf{\Sigma}\mathbf{K}_1^T + \mathbf{K}_2\mathbf{\Sigma}_\Theta\mathbf{K}_2^T \quad (9)$$

where $\mathbf{\Sigma}$ is a matrix consisting of the error variance matrix of the robots 1 and 2, and the error covariance matrix between the robots 1 and 2.

$$\mathbf{\Sigma} = \begin{pmatrix} \mathbf{\Sigma}_{11} & \mathbf{\Sigma}_{12} \\ \mathbf{\Sigma}_{21} & \mathbf{\Sigma}_{22} \end{pmatrix} \tag{10}$$

$\mathbf{\Sigma}_\Theta$ is

$$\mathbf{\Sigma}_\Theta = diag(\sigma_r^2\ \sigma_\phi^2\ \sigma_\psi^2) \tag{11}$$

and σ_r^2,σ_ϕ^2, and σ_ψ^2 are the error variances of distance, azimuth, and elevation angles, respectively. Note that the measurement error Θ is assumed to be obtained independently at each measurement, and thus it does not correlate with the previous positioning error $\mathbf{X}_{1,2}$.

Now we want to solve Eq.(7) to obtain the solution $\mathbf{X}_0$. Since the coefficient matrix $\mathbf{A}$ is not a square matrix, we solve Eq.(7) using the weighted least squares method. Firstly, we consider the residual equation.

$$\mathbf{V} = \mathbf{L} - \mathbf{A}\mathbf{X}_0 \tag{12}$$

Then, the error sum of squares weighted by $\mathbf{\Sigma}_L^{-1}$ shown in the following equation is minimized.

$$\min \mathbf{V}^T \mathbf{\Sigma}_L^{-1} \mathbf{V} \tag{13}$$

By substituting Eqs.(9) and (12) into Eq.(13) and differentiating it with respect to $\mathbf{X}_0$, the residual position of the robot 0, $\mathbf{X}_0$, which minimizes the error sum of squares is derived as follows:

$$\mathbf{X}_0 = (\mathbf{A}^T \mathbf{\Sigma}_L^{-1} \mathbf{A})^{-1} \mathbf{A}^T \mathbf{\Sigma}_L^{-1} \mathbf{L} = \mathbf{B}\mathbf{L} \tag{14}$$

In addition, the error variance matrix of the position of the robot 0 is derived from Eq.(14) as

$$\mathbf{\Sigma}_0 = \mathbf{B}\mathbf{\Sigma}_L\mathbf{B}^T = (\mathbf{A}^T \mathbf{\Sigma}_L^{-1} \mathbf{A})^{-1} \tag{15}$$

and the covariance matrices between the robots 0 and 1, and the robots 0 and 2 are obtained as

$$(\mathbf{\Sigma}_{01}, \mathbf{\Sigma}_{02}) = \mathbf{B}\mathbf{K}_1\mathbf{\Sigma} \tag{16}$$

Next, in the case that the child robot i moves and stops, and its position is identified by the parent robot as shown in Fig.1(2)(3), the position of the child robot is calculated as

$$x_i = x_0 + r_i \cos\phi_i \cos\psi_i \tag{17}$$

$$y_i = y_0 + r_i \sin\phi_i \cos\psi_i \tag{18}$$

$$z_i = z_0 + r_i \sin\psi_i \tag{19}$$

By substituting $x_i = \tilde{x}_i + dx_i$ into above equations and applying Taylor expansion, the following equation is obtained.

$$\mathbf{X}_i = \mathbf{L}_i + \mathbf{X}_0 + \mathbf{K}_{2,i}\mathbf{\Theta} \tag{20}$$

where $\mathbf{X}_i = (dx_i\ dy_i\ dz_i\ d\theta_i)^T$ and

$$\mathbf{L}_i = \begin{pmatrix} \tilde{x}_0 + \tilde{r}_i \cos\tilde{\phi}_i \cos\tilde{\psi}_i - \tilde{x}_i \\ \tilde{y}_0 + \tilde{r}_i \sin\tilde{\phi}_i \cos\tilde{\psi}_i - \tilde{y}_i \\ \tilde{z}_0 + \tilde{r}_i \sin\tilde{\psi}_i - \tilde{z}_i \end{pmatrix} \tag{21}$$

Therefore, the residual position of the child robot i, the error variance matrix, and the error covariance matrix are derived as the following equations.

$$\mathbf{X}_i = \mathbf{L}_i \tag{22}$$

$$\mathbf{\Sigma}_{ii} = \mathbf{\Sigma}_0 + \mathbf{K}_{2,i}\mathbf{\Sigma}_{\Theta_i}\mathbf{K}_{2,i}^T \tag{23}$$

$$\mathbf{\Sigma}_{0i} = \mathbf{\Sigma}_{ij} = \mathbf{\Sigma}_0 \tag{24}$$

Consequently, the positioning procedure is summarized as follow: i) assume the proper initial position of robot i as $\tilde{\mathbf{P}}_i$ and calculate $\mathbf{X}_i$ by solving Eqs.(14) and (22), ii) substitute $\tilde{\mathbf{P}}_i \leftarrow \tilde{\mathbf{P}}_i + \mathbf{X}_i$, ii) repeat (i) and (ii) until $\mathbf{X}_i$ becomes small enough. The positioning accuracy after repeating the position identification by CPS can be estimated by calculating the error variance and covariance matrices according to Eqs.(15), (16), (23), and (24).

As an example, we substituted the actual measurement error of the laser range finer explained in Section III ($\sigma_r = 3[mm], \sigma_\phi = 5[sec.]$, and $\sigma_\psi = 5[sec.]$), and calculated the positioning error after 1km movement. CPS motion in Fig.1 is repeated 100 times and the robots moved 10m in one cycle, respectively. The obtained positioning accuracy was $\sigma_x^2 + \sigma_y^2 = 0.0203[m^2]$ for the position elements of the error variance matrix of the parent robot 0, $\mathbf{\Sigma}_0$. In actual scenario, due to the measurement error of the body inclination or the offset of the center position of corner cubes, such a high precision cannot be achieved. However we have confirmed that incomparable highly precise positioning is possible against conventional dead reckoning method which utilizes the rotation angle of wheels [6].

3 Construction of 3D environmental map by multiple robots

This section proposes a new measurement system for precise construction of a 3D environmental map by combining CPS for multiple robots and a laser range finder. In this system, mobile robots move around a large scale target and scan the target by an on-board 3D laser range finder from several viewpoints. Each measurement position is identified by CPS precisely using a parent and two child robots. Since there is no need to apply laborious post-processing procedures, the whole picture of the large scale architecture can be obtained with ease and high accuracy. Firstly, we introduce the fifth CPS machine model named CPS-V, which is equipped with a 2D laser range finder and a scanning mechanism, and show experimental results for the construction of indoor and outdoor environmental maps by CPS-V.

3.1 The fifth CPS machine model, CPS-V

Figure 4 shows the fifth CPS machine model named CPS-V. This system consists of a parent robot (P-cle, Parent mobile unit, Fig.6) and two child robots (HPI Japan, Fig.5). The parent robot is equipped with the on-board 2D laser range finder (LMS 200, Sick), a high precision 2-axis attitude sensor (MD900T, Applied Geomagnetics), and a total station for surveying (AP-L1, TOPCON Ltd.)(Table 1) which is used for measuring relative positions from the child robots. Even if the body is tilted on a slope, body inclination can be compensated by the attitude sensor and precise positions of the robots can be identified. The 2D laser range finder can acquire slit-like range data within the range of 80m and 180 degrees as shown in Table 2. The parent robot has a rotating table on the upper body, and by rotating the table around the vertical axis while scanning by the 2D laser range finder, all around 3D range images from the parent robot can be acquired in 37.8 seconds.

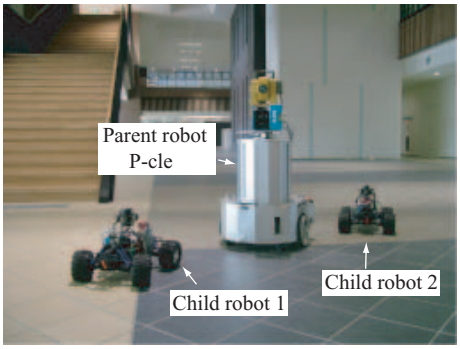

Figure 4. Fifth CPS machine model, CPS-V

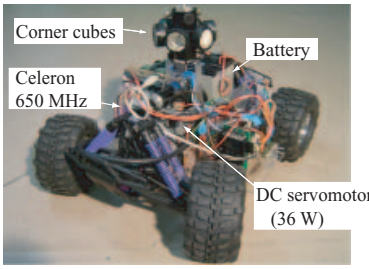

Figure 5. Child robot

3.2 Construction experiment of indoor environmental map

Experiments for constructing 3D maps are carried out using CPS-V in an indoor environment.

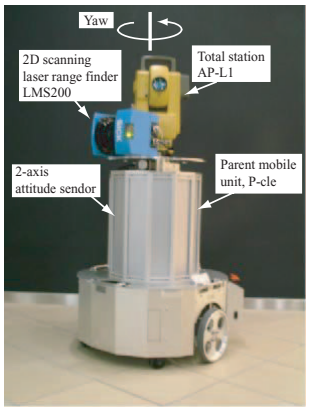

Figure 6. 3D laser measurement using rotation table around Yaw axis

AP-L1 (TOPCON Ltd.)	
Range	$4 \sim 400$[m]
Resolution (distance)	0.2[mm]
Resolution (angle)	5”
Precision (distance)	$\pm$ 3+2ppm[mm]
Precision (angle)	$\pm$5”

Table 1. Specification of total station, AP-L1

In this experiment, each robot moves 4m at a time and the parent robot captures 3D range images at each static position by rotating the on-board 2D laser range finder around the vertical axis (Fig.7). Obtained range images are transformed to the world coordinate system by simple coordinate transformation calculation using the measured position by CPS. No post-processing procedure such as ICP algorithm is applied.

Path of the parent robot is shown in Fig.8. The parent robot moved up to 39m in x-direction and 10m in y-direction in the hall. Obtained 3D environmental maps are shown in Figs.9 and 10. Circles in the 3D range images indicate the measurement positions of the parent robot. The parent robot captured the range images 23 times during the movements in the hall. Total distance traveled by the parent robot is 86.21m. From these results, it is confirmed that, without post-processing procedures such as ICP, 3D environmental maps in unknown environment can be easily obtained by applying simple coordinate transformation using position information measured by CPS. The difference of measured positions of the corner indicated in Fig.8 before and after the movements is 1.17m (1.36% of the distance traveled). This error is fairly larger than the results obtained by CPS so far. One of the reasons is that relative distances between robots were about 4m, and this value is the measurement limit of the laser range finder as shown in Table

LMS 200 (SICK Corp.)	
Range	80[m]
Field of view	180°
Resolution (distance)	10[mm]
Resolution (angle)	0.5°

Table 2. Specification of laser range finder, LMS200

Figure 7. 3D laser measurement using multiple robots

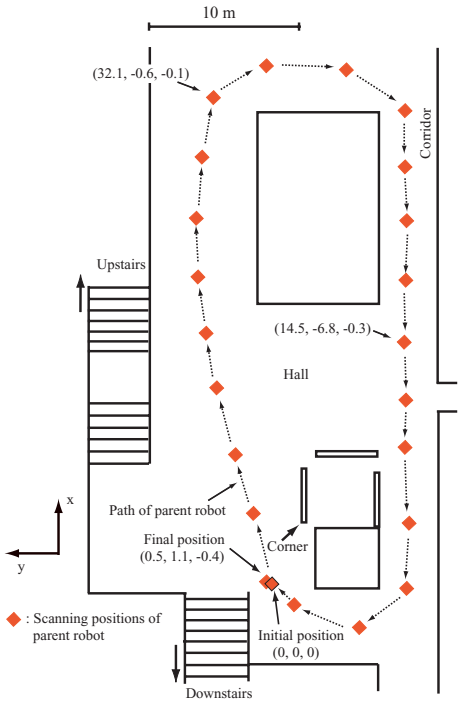

Figure 8. Path of parent robot

2. From error measurement experiments of this sensor, it is known that measurements for short distances tend to contain large distance errors, and the distance error is almost uniform for the measurement from 10m to 70m. Thus, if the robots keep larger relative distances between them, and moves longer distance at one cycle, the accuracy is expected to be higher than the results obtained by this experiments. In addition, after the Step (3) in Fig.1, the parent robot can move, stop, and measure the environment repeatedly while the child robots keep stationary. This strategy can reduce the number of CPS cycle and the measurement accuracy may be greatly improved when the robots work in a large area.

3.3 Construction experiment of large scale outdoor environmental map

Next, we performed the construction experiment of 3D environmental maps of large scale architecture. We measured outward walls of a building from 13 points in outdoor environment and constructed 3D models of the building. Path of the parent robot and obtained maps are shown in Figs.8 and 13. In this experiment, we used small number of measurements from sparse view points, and neither dense range data nor sufficient overlapped regions, which are indispensable for applying ICP algorithm, were available. From this experiment, we can conclude that it is possible to construct 3D maps of simple but large scale architecture by the proposed system with few scanning times. The positioning error in this experiment is 0.63m against the total travel distance of the parent robot of 147.7m, which is 0.43% of the distance traveled.

4 Conclusions

This paper proposed a new 3D measurement system for large scale architectures using the precise positioning system by multiple robots named CPS and an on-board laser range finder. This system needs no post-processing procedures such as ICP algorithm, and can be applied to sparse range measurements. Therefore, there is a possibility to realize a fully automatic 3D measurement system for large scale architecture such as large cultural heritages with the proposed system. The measurement experiments in unknown and large indoor/outdoor environments are successfully carried out using the newly developed multiple robots system named CPS-V.

Our future works include the development of the automatic 3D laser measurement system which selects optimum measurement points automatically instead of operator's command. The positioning accuracy of CPS can also be improved by the back-projection technique, that is, the observation of some stable landmarks before and after the

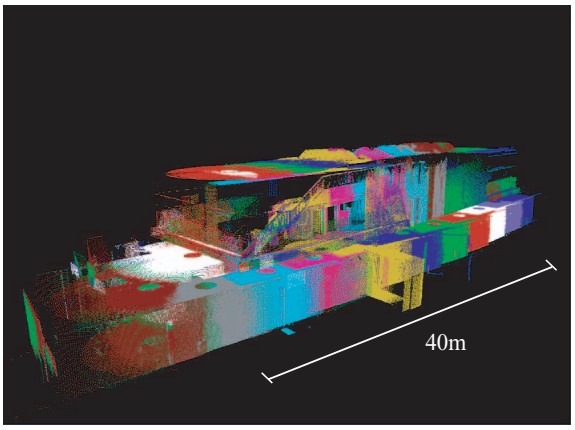

Figure 9. Obtained 3D map of indoor environment

movements and the correction of each measurement position by back-projecting errors. Combination of CPS with ICP method depending on the situations is also worth considering in order to improve the accuracy of both positioning and obtained 3D environmental maps.

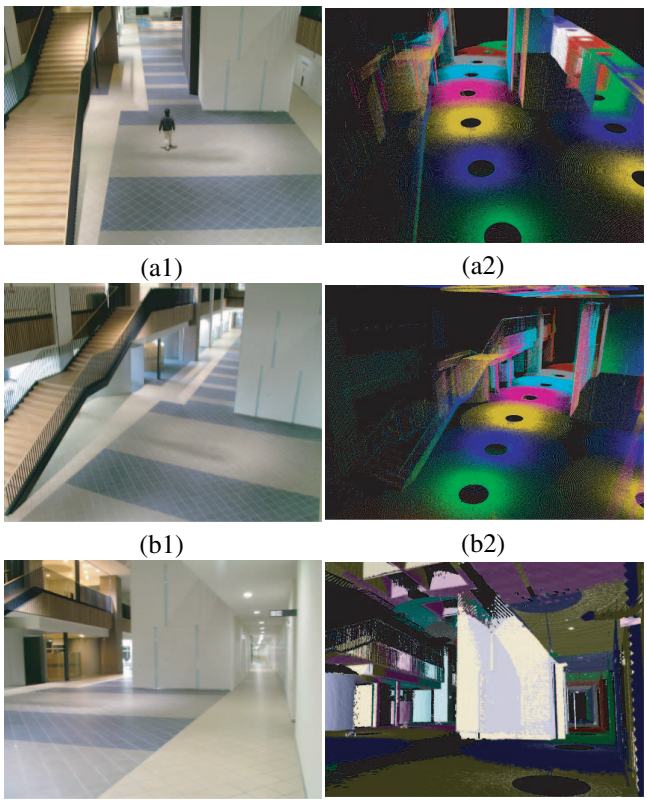

Figure 10. Obtained 3D map of indoor environment

References

[1] Toppan vr system. *http://biz.toppan.co.jp/vr/*.

[2] P. J. Besl and N. D. McKay. A method for registration of 3-d shapes. *IEEE Transactions on Pattern Analysis and Machine Intelligence*, 2(14):239–256, 1992.

[3] Y. Chen and G. Medioni. Object modelling by registration of multiple range images. *Image and Vision Computing*, 3(10):145–155, 1992.

[4] D. M. Cole and P. M. Newman. Using laser range data for 3d slam in outoor environment. *Proc. IEEE International Conference on Robotics and Automation*, pages 1556–1563, 2006.

[5] K. Ikeuchi, K. Hasegawa, A. Nakazawa, J. Takamatsu, T. Oishi, and T. Masuda. Bayon digital archival project. *In Proceedings of the Tenth International Conference on Virtual System and Multimedia*, pages 334–343, November 2004.

[6] R. Kurazume and S. Hirose. An experimental study of a cooperative positioning system. *Autonomous Robots*, 8(1):43–52, 2000.

[7] R. Kurazume, S. Nagata, and S. Hirose. Cooperative positioning with multiple robots. *Proc. IEEE Int. Conf. on Robotics and Automation*, 2:1250–1257, 1994.

[8] M. Levoy, K. Pulli, B. Curless, S. Rusinkiewicz, D. Koller, L. Pereira, M. Ginzton, S. Anderson, J. Davis, J. Ginsberg, J. Shade, and D. Fulk. The digital michelangelo project: 3d scanning of large statues. *Proc. ACM SIGGRAPH 2000*, pages 131–144, July 2000.

[9] A. Nuchter and H. Surmann. 6d slam with an application in autonomous mine mapping. *Proc. IEEE International Conference on Robotics and Automation*, pages 1998–2003, 2004.

[10] K. Ohno, T. Tsubouchi, and S. Yuta. Outdoor map building based on odometory and rtk-gps positioning fusion. *Proc. IEEE International Conference on Robotics and Automation*, pages 684–690, April 2004.

[11] J. Weingarten and R. Siegwart. Ekf-based 3d slam for structured environment reconstruction. *Proc. IEEE/RSJ International Conference on Intelligent Robots and System,*, pages 2089–2094, 2005.

[12] H. Zhao and R. Shibasaki. Reconstructing a textured cad model of an urban environment using vehicle-borne lase range scanners and line cameras. *Machine Vision and Applications*, 14:35–41, 2003.

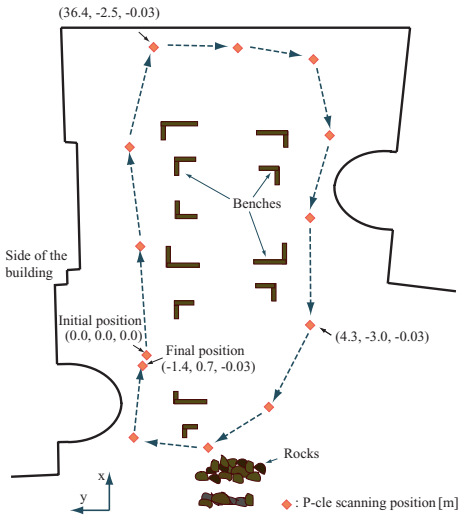

Figure 11. Path of parent robot

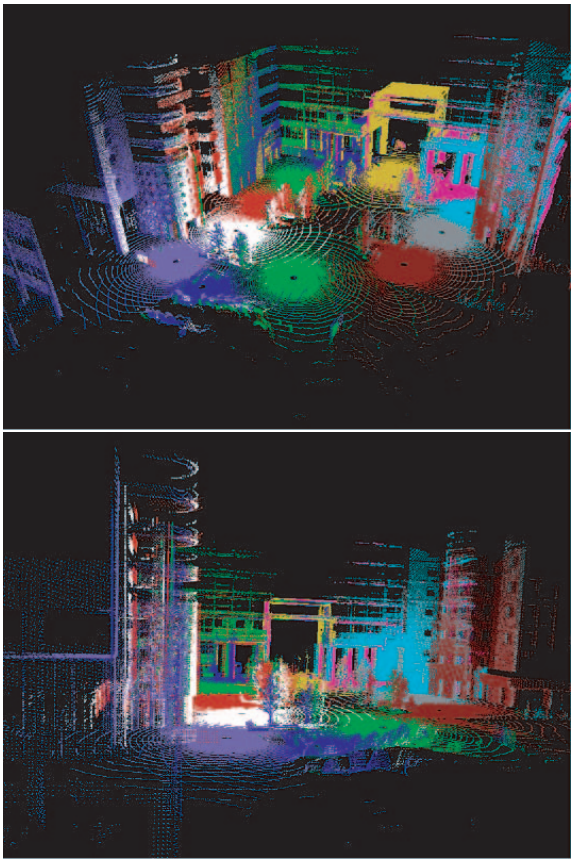

Figure 12. 3D map of buildings in outdoor environment

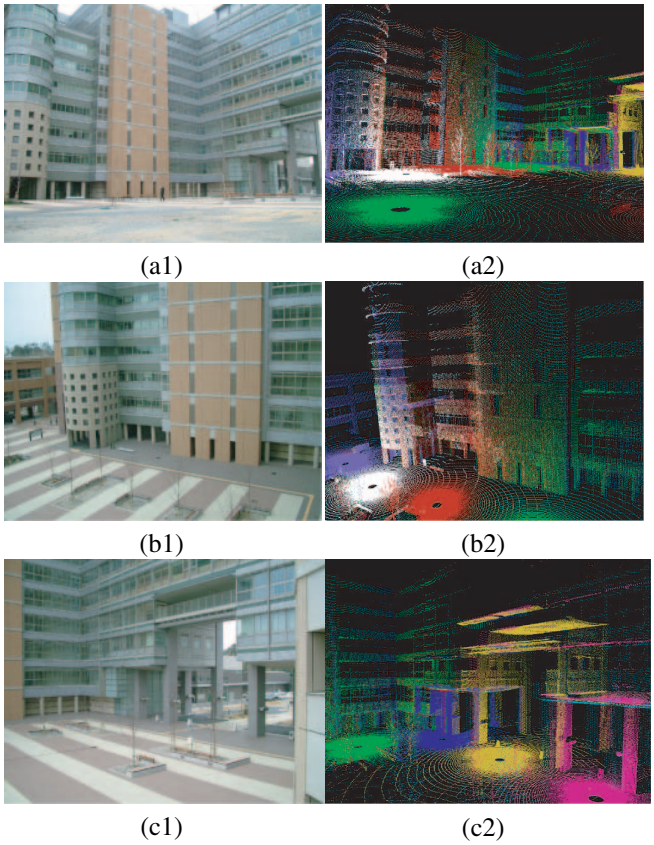

Figure 13. 3D map of buildings in outdoor environment